

Fundamental Studies on a New Series of SPSEBS-PVA-QPSEBS Bipolar Membrane: Membrane Preparation and Characterization

Krishnaveni Venugopal, Sangeetha Dharmalingam

Department of Chemistry, Anna University, Sardar Patel Road, Chennai 600025, Tamil Nadu, India

Correspondence to: S. Dharmalingam (E-mail: sangeetha@annauniv.edu)

ABSTRACT: A sulfonated polystyrene ethylene butylene polystyrene (SPSEBS)-poly(vinyl alcohol) (PVA)-Quaternized polystyrene ethylene butylene polystyrene (QPSEBS) bipolar membrane (BPM) was prepared by lamination method using PSEBS as the starting material, the functionalization of which was modified by sulfonation and amination while PVA was used as the intermediate layer to enhance the water splitting efficiency. The cross section view of SPSEBS-PVA-QPSEBS BPM was studied by SEM. Fourier transform infra-red spectroscopy (FTIR) studies indicated that the prepared BPM contained $-\text{SO}_3^-$, $-\text{NR}_3^+$, and $-\text{C}-\text{N}$ functional groups. The thermal stability of the prepared BPM was studied by thermogravimetric analysis (TGA). Some of the BPM characteristics results showed that the co-ion fluxes was greater for t_{Cl^-} (0.065) when compared with t_{Na^+} (0.051) along with a water splitting capacity value of 0.88 for SPSEBS-PVA-QPSEBS BPM. The water dissociation flux was 2.8×10^{-5} mol/m²/s and 2.2×10^{-5} mol/m²/s for the acid (H^+) and base (OH^-), respectively. The other essential current-voltage characteristics and permeate flux across the membrane were also evaluated. © 2012 Wiley Periodicals, Inc. *J. Appl. Polym. Sci.* 000: 000–000, 2012

KEYWORDS: bipolar membrane electrodialysis; polyvinyl alcohol interface; water splitting capacity; current-voltage curve

Received 7 March 2012; accepted 20 May 2012; published online

DOI: 10.1002/app.38098

INTRODUCTION

Desalination using electrically driven processes such as electro-dialysis (ED) and water splitting ED using ion exchange membrane (IEM) are considered as viable options for producing potable water from brackish and sea water in many parts of the world, as the average per capita supply of clean water is expected to decrease by one-third in the next 20 years.¹ Remarkable improvements in desalination processes have rendered them more reliable with reduced capital costs.^{2,3} ED is a simple IEM separation process which uses electrical potential as the driving force for separation. It can be used as a single unit operation and combined with other processes for treating different types of wastes. As the temperature does not influence the rate of separation of salt from feed solution, it is possible to operate ED continuously. These stated advantages render ED highly attractive, especially for desalination of brackish water as well as for the production of table salt and organic acids.^{4,5} Although commercially available membranes with excellent properties are widely marketed in the world, there is a growing demand for membranes that are ecofriendly, easier to prepare and less expensive with hydrophilic characteristics.⁶ In the literature, many works have been reported with respect to the preparation of composite membranes by surface modification of ceramic supports using a thin polymer coating resulting in

controlled permeability characteristics and improved barrier performance in terms of flux and selectivity over the commercial membranes.⁷ Among all, BPMs comprise an important area of membrane research. Industrial chemistry involves a large number of neutralization reactions, such as acids which react with bases to form salts and water. However, most of the salts have no commercial value and are discharged into the environment resulting in environment pollution. In the light of this pollution, the ideal solution is to convert the salt and water back into acid and base with the help of a BPM.⁸ BPMs have been used in industries for pollution control, resource recovery, and chemical processing with a simple process, high efficiency, and low waste disposal. Usually, a BPM is composed of a cation exchange layer (CEL), an anion exchange layer (AEL), and an intermediate layer (IL, the layer between the cation and the anion layers).⁹ With the help of an electrical field, protons and hydroxide ions are generated by water splitting at the interlayer and migrate into the cathode and the anode chambers, respectively.

However, the techniques used in the preparation of BPM present certain limitations in practically using them for various applications. Recently, great attention has been paid to the modification of CEL or AEL and the introduction of catalytic IL to promote water splitting. Different types of ILs were used

to catalyze the water dissociation by various investigators which included (i) a matrix material containing quaternary and non-quaternary amine group, weak acid and its corresponding base; (ii) inorganic substances having amphoteric characteristics such as sodium meta silicate, ruthenium trichloride, metal oxides, and zeolite; (iii) noble metal ions/heavy metal ions such as Ag^+ , Fe^{2+} , Fe^{3+} , Ti^{4+} , Sn^{2+} , Pd^{2+} , Ru^{3+} etc; (iv) macromolecules like polystyrene, polycarbonate, polyvinyl alcohol, polyethylene glycol, bovine serum albumin, polyamidoamine dendrimer, etc., have also been reported.¹⁰ In general, BPM can be prepared by two different techniques. One is through single sheet method in which, one side of the membrane is selectively functionalized to give cation selectivity while the other side is functionalized to give anion selectivity. The second technique is lamination which involves either hot pressing using heat and pressure or gluing using an adhesive paste or by means of casting anionic polyelectrolyte paste/solution on a commercially available cationic exchange membrane (CEM) or vice versa.¹¹

Some investigators such as Yang et al., have developed a BPM and reported their studies on the various applications using BPM technology.¹² However, there is still a lacunae in the performance between laboratory-prepared membranes and commercial membranes. Furthermore, the domestic studies mainly focused on the application rather than membrane fabrication, and hence, only a few studies on preparation have been reported.^{13,14} The preparation of an adequately functional BPM requires the optimization of its different components. The choice of a suitable preparation route for the desired materials should be part of this optimization. In this study, a hydrocarbon thermoplastic elastomer PSEBS (polystyrene ethylene butylene polystyrene), was used for the preparation of CEL, AEL, and BPM. The aim of this work was to prepare and characterize a laminated sulfonated polystyrene ethylene butylene polystyrene (SPSEBS)-poly(vinyl alcohol)(PVA)-Quaternized polystyrene ethylene butylene polystyrene (QPSEBS) BPM with good thermal stability by sulfonation and amination functionalization with PVA as IL to enhance the water splitting efficiency.

EXPERIMENTAL

Materials

Poly (styrene ethylene butylene polystyrene) triblock copolymer was purchased from Aldrich, India with the reported properties: $M_w = 89,000$, $M_w/M_n < 1.06$ and 28.6 wt % styrene unit. Chlorosulphonic acid (CSA) was obtained from Spectrochem, India. While Tributyl phosphate (TBP) was procured from Lancaster and Tetrahydrofuran (THF) was obtained from Merck, India. Chloroform, Triethyl amine (TEA), concentrated Hydrochloric acid (HCl), and Zinc chloride were purchased from Sisco Research Laboratory, India. PVA ($M_w = 14,000$) and paraformaldehyde were purchased from Central Drug House, India. All the chemicals were of analytical grade and used as received.

Preparation of the SPSEBS-PVA-QPSEBS BPM

Preparation of CEL. For the preparation of the CEL, the weighed PSEBS polymer was dissolved in chloroform at 0.0°C to which, required amounts of TBP (moderator) followed by CSA (drop wise over a period of time) were added under nitrogen atmosphere with continuous stirring. After 3 h, the reaction

was terminated using methanol to obtain sulfonated PSEBS (SPSEBS). CEL was obtained by dissolving SPSEBS ionomer in THF solution which was then casted on a petri dish and the solvent allowed to evaporate. The schematic diagram of preparation of CEL of SPSEBS-PVA-QPSEBS BPM is given in Figure 1. The thickness of the membranes was controlled in the range of 25–30 μm . The amount of sulfonic acid group present in the SPSEBS ionomer was determined quantitatively by volumetric method. Initially, 0.1 g of SPSEBS ionomer was taken and equilibrated in 20 mL of standard sodium carbonate solution of 0.01 M. Then the solution was filtered and the filtrate washed with distilled water followed by titration against known concentration of HCl solution using methyl orange as indicator. The titer value was noted once the orange color end point was reached and the blank experiment without the ionomer concentration was conducted with the same experimental set up and the titer value for the blank was also noted. The differences between both the titer values represented the amount of sulfonic acid group present quantitatively in the given gram of sample. The amount of sulfonic acid group concentration was found to be 1.356 meq/g of the SPSEBS ionomer.

Preparation of AEL. The AELs were prepared by dissolving PSEBS in chloroform to which conc. HCl was added drop wise with continuous stirring followed by paraformaldehyde as a chloromethylating agent while zinc chloride was added as a Lewis acid catalyst. The reaction was maintained at 60°C . After 48 h, the reaction was terminated using methanol. The above obtained chloromethylated PSEBS (CMPSEBS) was dissolved in THF and to this required amount of TEA solution was added and maintained at 60°C in nitrogen atmosphere throughout the reaction. After 48 h, the reaction was terminated and AEL was obtained by solution casting method. The schematic diagram of preparation of AEL of SPSEBS-PVA-QPSEBS BPM is given in Figure 1. The amount of Quaternary amine group present in the QPSEBS ionomer was determined quantitatively by volumetric method. Initially, the blank experiment was done using known amount of prepared standard silver nitrate solution against known volume of excess potassium thiocyanate solution in the presence of nitric acid (1+1) solution to acidify the solution so as to avoid the formation of $\text{Fe}(\text{OH})_3$. Ammonium ferric sulfate solution was used as an indicator to identify the end point. However, the use of acidic medium together with added SCN^- titrant increases the solubility of the precipitate. To avoid this, nitrobenzene or chloroform was added as it surrounds the precipitate and shields it from coming in contact with the added SCN^- solution. The content was shaken well for about 10 min to flocculate the precipitate. The titrate remained pale yellow as the excess (unreacted) silver ions reacted with the thiocyanate ions to form a silver thiocyanate precipitate. Once all the silver ions were reacted, the slightest excess of thiocyanate reacts with Fe^{3+} to form a dark red complex. At this point, the titer value was noted for the blank sample. Before this titration, an excess volume of silver nitrate solution was added to the solution containing chloride ions of known concentration, forming a precipitate of silver chloride. The term “excess” is used as the moles of silver nitrate added are known to exceed the moles of sodium chloride present in the sample so that all the chloride ions present will react.

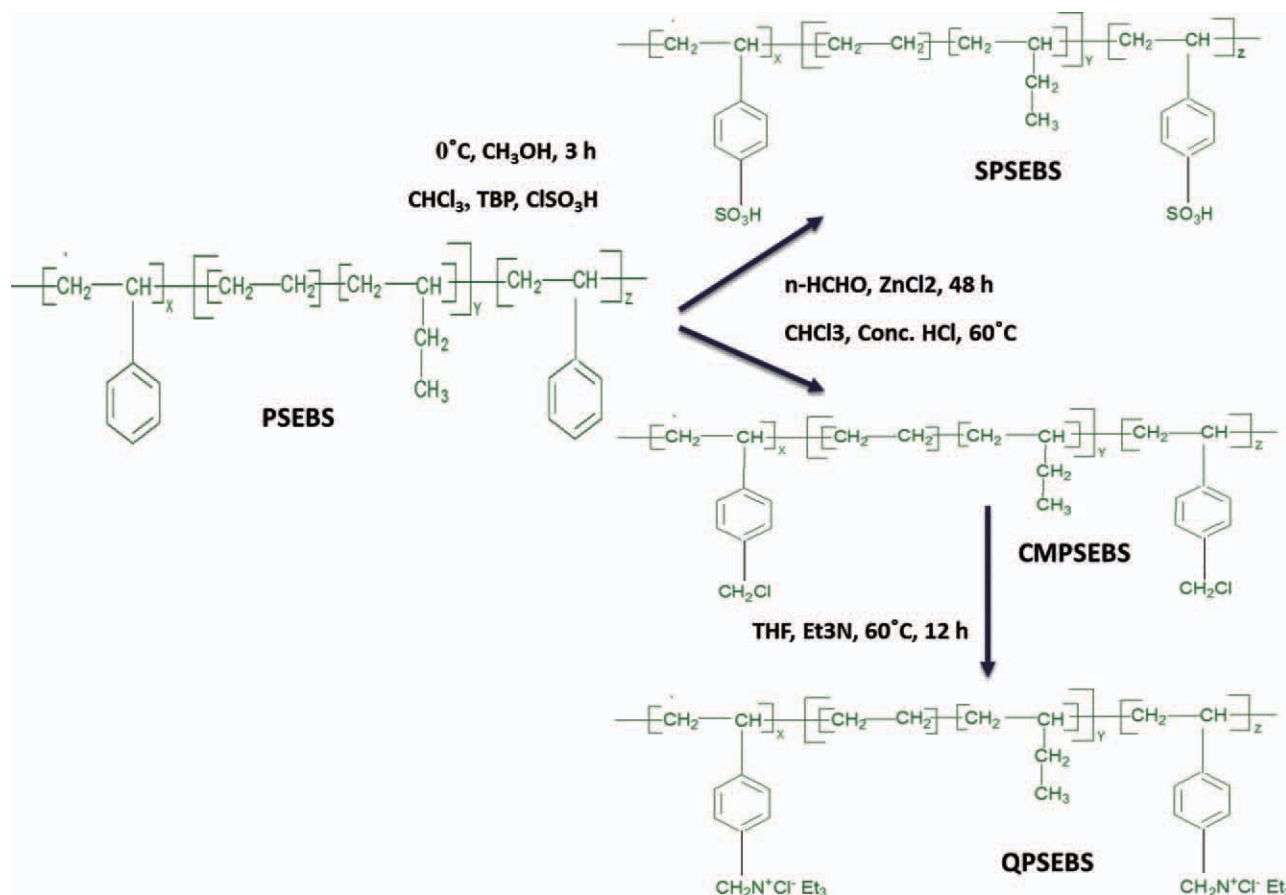


Figure 1. Schematic diagram of preparation of AEL and CEL of SPSEBS-PVA-QPSEBS BPM. [Color figure can be viewed in the online issue, which is available at wileyonlinelibrary.com.]

The concentration of chloride ions was determined by subtracting the titration findings of the moles of silver ions that reacted with the thiocyanate from the total moles of silver nitrate added to the solution. Initially, 0.1 g of QPSEBS ionomer was taken and equilibrated in sodium hydroxide solution of known concentration. To this solution, an excess volume of a silver nitrate solution was added and the remaining steps followed were similar as that explained for blank sample. The differences between both the titer values represented the amount of quaternary amine group present quantitatively in the given gram of sample. The amount of quaternary amine group concentration was found to be 0.892 meq/g of the SPSEBS ionomer.

BPM Preparation. The AEL and CEL were individually prepared by casting method, cut to $10 \times 12 \text{ cm}^2$ size and washed repeatedly with 1M NaOH followed by 1M HCl acid aqueous solutions for at least three times. Subsequently, the AEL was equilibrated with 2 M NaCl solution so as to transform it into chloride form which was then washed with distilled water and dried. BPM was prepared by bonding together the separate anion and CELs. The two monopolar membranes of opposite selectivity were fused together with PVA macromolecule as the IL due to its properties of being linear and hydrophilic. PVA was additionally expected to display hydrogen bonding as well as polar interactions with water molecules. The above described

fusion was carried out in a hydraulic press for 5 min at a temperature of about 64°C and pressure of about 3 ton. The thickness of the prepared BPM was found to be $50\text{--}60 \mu\text{m}$.

Membrane Characterization

Instruments. The structural conformations of the prepared membranes were done using Fourier transform infra-red spectroscopy (FTIR) techniques. The IR spectra ($450\text{--}4000 \text{ cm}^{-1}$) for the dried membranes were recorded in transmission mode using Perkin Elmer FTIR spectrometer at $25 \pm 2^\circ\text{C}$ by placing the membranes in KBr windows. The thermogravimetric analysis (TGA), performed using a SDT Q600 US analyzer, was carried out to determine the thermal stability of the membranes. The loss in weight of the membranes with increase in temperature from room temperature (30°C) to 800°C at a heating rate of $20^\circ\text{C}/\text{min}$ under nitrogen atmosphere was studied. The surface morphology of the membranes was analyzed by scanning electron microscope (SEM) (Hitachi S-3400 N model). The samples were cut into sufficient size and sputter coated with gold to make the samples electro conductive. The samples were then analyzed under vacuum condition at an accelerating voltage of 10 kV.

Determination of Water Absorption, IEC, and C_R . Uptake of water enhances the ionic conductivity of the membranes. Water absorption study of the membranes was carried out by

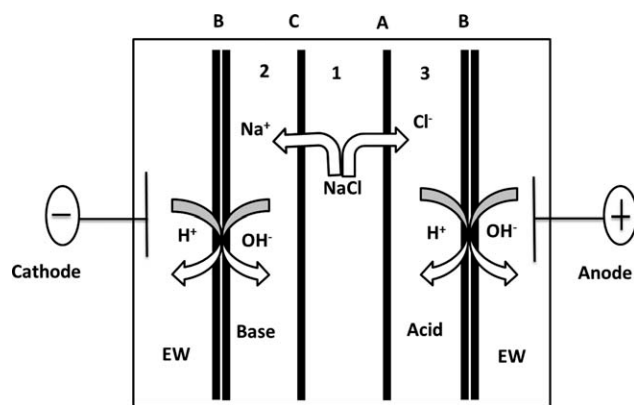


Figure 2. Schematic diagram of five compartment electrodiolytic cell configuration for measuring current-voltage relationship and evaluating water dissociation capacity for BPMs.

measuring the change in weight of the membranes before and after hydration. The OH^- and H^+ forms of the membranes were immersed in deionized water at room temperature and equilibrated for more than 24 h. The percentage of water absorbed was calculated using the following relation.

$$\text{Water absorption(\%)} = \frac{\text{Weight of the wet membrane} - \text{weight of the dry membrane}}{\text{Weight of the dry membrane}} \times 100 \quad (1)$$

The ion exchange capacity (IEC) values of the CEL and AEL were calculated by titration method. Greater the IEC better will be the ionic conductivity of the membrane. The preweighed CEL was soaked in excess of KCl salt solution to extract all protons from the membrane. The electrolyte solution was then neutralized using Na_2CO_3 solution of known concentration with phenolphthalein as indicator. The IEC value of AEL was determined by Argentometric titration method. The membrane was weighed and then soaked in water to extract all the Cl^- from the membrane. After 24 h, the solution was titrated against AgNO_3 in the presence of K_2CrO_4 as indicator. The fixed group concentration (C_R) was determined directly from the ratio of IEC to water absorption and expressed in M (mol/L).

$$\text{IEC} = \frac{\text{Titre value (mL)} \times \text{Normality of titrant (N)}}{\text{Weight of the dry polymer membrane (g)}} \text{ meq/g} \quad (2)$$

Determination of co-ion Fluxes and Water Splitting Capacity. The schematic diagram of the experiment for determining the flow of Na^+ and Cl^- ions through a BPM is indicated in the Figure 2 which represents an ED stack consisting of five individual cells for water dissociation and to convert the salt into corresponding acid and base, respectively. The effective membrane area was 120 cm^2 . Parallel-cum-series flow arrangement was used for each compartment separately. Peristaltic pumps were used to feed NaCl solution (50 g/L) in recirculation mode into the respective compartments. The anode used was Ti-based metal coated with Ti-Ru-Pd oxides and the cathode was made of stainless steel. Constant applied voltage across the electrodes was applied by DC power supply and the resulting

current variation was recorded as a function of time. The whole setup was placed at ambient condition (303 K) without any additional temperature control. 0.05 M NaCl solution was recirculated through the electrode compartments as electrode wash, while salt solution was initially fed into compartment 1, and distilled water was fed into compartments 2 and 3. When the entire ED cell was under electric field using electrodes, the large electric field appearing at the membrane interface produces an excess of OH^- and H^+ ions due to the field enhanced chemical reaction. These water ions permeate the corresponding exchange layers of the BPM and enter into the adjacent solutions resulting in the formation of acid and base. The pH and conductivity of each output stream were regularly monitored. The co-ion flows were estimated by measuring the rates of accumulation of the ions in the various compartments during current flow. The acid and alkaline solutions were then withdrawn from their compartments and analyzed for Na^+ and Cl^- ions respectively.

The experiment of co-ion leakage through SPSEBS-PVA-QPSEBS BPM and water splitting capacity of BPM was carried out according to the procedures reported in the literature.^{15,16}

$$t_{\text{Na}^+(\text{Cl}^-)}^{\text{BPM}} = F \frac{C_i V_t - C_i V_i}{I t} \quad (3)$$

$$r_{\text{diss}}^{\text{BPM}} = 1 - (t_{\text{Na}^+}^{\text{BPM}} + t_{\text{Cl}^-}^{\text{BPM}}) \quad (4)$$

where, $t_{\text{Na}^+(\text{Cl}^-)}^{\text{BPM}}$ is the transport number of chloride or sodium through the BPM; $r_{\text{diss}}^{\text{BPM}}$ is the current efficiency of the water dissociation; F is the Faraday constant (96,500 C/mole); $C_i V_i$ and $C_i V_t$ are the concentrations and volume of sodium or chloride in the compartment at the initial time and time at t , respectively.

Determination of Permeate Flux, Water Dissociation Flux, and C-V Curve. The permeate flux (F)¹⁷ and water dissociation flux ($J_{\text{H}^+ \text{ or } \text{OH}^-}$)¹⁶ across the membrane can be calculated by

$$F = \frac{J(L)}{A(\text{m}^2) \times T(\text{h})} (\text{L}/\text{m}^2/\text{h}) \quad (5)$$

$$J_{\text{OH}^- \text{ or } \text{H}^+} = \frac{V \times \left(\frac{dC_{\text{OH}^- \text{ or } \text{H}^+}}{dt} \right)}{A} \quad (6)$$

where, J is the volume of the permeate flux; A is the surface area of the membrane; T is time; V is the total volume; A is the effective membrane area; and $\frac{dC_{\text{OH}^- \text{ or } \text{H}^+}}{dt}$ is the change in acid (H^+) or base (OH^-) concentration in compartments (2 or 3) with time.

The measurements of the current-voltage response for SPSEBS-PVA-QPSEBS BPM were taken in a laboratory-scale test cell designed with five-compartment for the production of acids and bases from their corresponding salts, which is one of the main applications of BPMs. Figure 2 shows the schematic representation of BPM ED system used. The water dissociation capabilities of the BPMs were evaluated through the five-compartment electrodiolytic cell experiments. The water dissociation capabilities measured in terms of water dissociation flux ($\text{mol s}^{-1} \text{ m}^{-2}$) was indicated by the number of protons on the surface of IEM during the experiments. In the cell stack

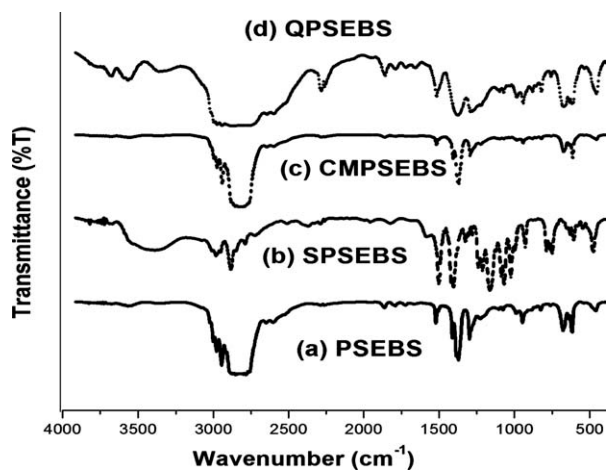


Figure 3. FTIR spectra of PSEBS (a), SPSEBS (b), CMPSEBS (c), and QPSEBS (d).

configurations, illustrated in Figure 2, each compartment was separated by the membranes. Sodium chloride solution was used as the electrolyte solution and a current/voltage was supplied by a power supply into the membrane cell during the test. The cathode and anode were stainless steel and Ti-Ru- Pd oxides electrodes, respectively.

RESULTS AND DISCUSSION

FTIR Analysis

The infrared spectrum of PSEBS, SPSEBS, CMPSEBS, and QPSEBS are shown in Figure 3. In Figure 3 (a) the presence of bands at 3026 cm^{-1} and 758 cm^{-1} was due to the aromatic $\nu_s(\text{C-H})$ and $\delta(\text{C-H})$ vibrations, respectively. Appearance of transmission peaks at 2933 cm^{-1} and 2865 cm^{-1} were assigned to the aliphatic $\nu_{as}(\text{C-H})$ and $\nu_s(\text{C-H})$ vibrations, respectively. The peaks at 1363 cm^{-1} and 1430 cm^{-1} were due to the aromatic $\nu_s(\text{C=C})$ vibration. In Figure 3(b) the presence of a broad band around the wavenumber of 3435 cm^{-1} was assigned to the OH stretching of the sulphonic acid in the aromatic ring. The absorption bands at 1389 cm^{-1} and 1496 cm^{-1} were assigned to $\nu_{as}(\text{SO}_2)$ and this confirmed the sulphonation of the phenyl ring. The transmission peak at 1164 cm^{-1} was attributed to $\nu_{as}(\text{SO}_3)$ of sulphonic acid. The peaks at 720 cm^{-1} and 647 cm^{-1} were due to stretching of C-S and S-O vibration. In Figure 3(c), as a result of chloromethylation reaction, the peak at 687 cm^{-1} indicated the presence of monosubstituted benzene ring and peak at 1284 cm^{-1} was attributed to CH_2Cl group at the phenyl ring. In Figure 3(d), appearance of peak around 1257 cm^{-1} was assigned to C-N stretching vibration of aminated membrane. The broad peak at 2729 cm^{-1} was assigned as the characteristic peak for quaternary ammonium group.¹⁸ From the above discussion it was clear that sulphonation and amination reactions had occurred in the phenyl ring corresponding to CEM and anionic exchange membrane (AEM).

TGA Analysis

The TGA curves for all the synthesized membranes are shown in the Figure 4. The TGA curve of pristine PSEBS, as observed in Figure 4(a), exhibited a one stage degradation step that

occurred around 424°C due to the degradation of polymer main chain. TGA curve of SPSEBS shown in Figure 4(b), displayed two stages of degradation. The first weight loss was observed between 243°C and 290°C which could be due to the splitting of sulfonic acid groups from the polymer chain. The second weight loss observed above 412°C was due to the decomposition of polymer backbone.^{19,20,21}

TGA curve of QPSEBS, as observed in Figure 4(c), also exhibited two stages of degradation. The first weight loss that was observed above 200°C was due to the removal of quaternary ammonium groups from the polymer backbone. The second weight loss observed at temperatures above 400°C was due to the degradation of polymer main chain.^{22,23} In the case of BPM, as depicted in Figure 4(d), the degradation was observed to occur in four steps. The first weight loss was observed between 100°C and 160°C and was probably due to the removal of the physically and chemically bonded water along with trace amounts of solvent. The second weight loss that occurred beyond 200°C was attributed to the degradation of the functional groups (sulfonic acid and quaternary ammonium groups) from the polymer chain. Third weight loss that occurred after 300°C was attributed to the degradation of the intermediate PVA molecules. The fourth weight loss that occurred after 430°C was attributed to the main chain degradation.

Morphological Analysis

The cross sectional SEM images of PSEBS, SPSEBS, QPSEBS, BPM membranes are given in Figure 5(a, b, c, and d) respectively. It was observed from Figure 5(a, b, and c) that the individual polymer membranes showed a uniform, clear, and smooth surface which were densely packed and defect free. On the other hand, Figure 5(d) clearly showed three distinct regions. The top layer was the sulfonated polymer while the middle one represented the intermediate PVA. The last layer (third layer) corresponded to the quaternized polymer material. The surface view of PVA coated on SPSEBS, as given in Figure 5(e), confirmed the adsorption of PVA on the surface of the SPSEBS.

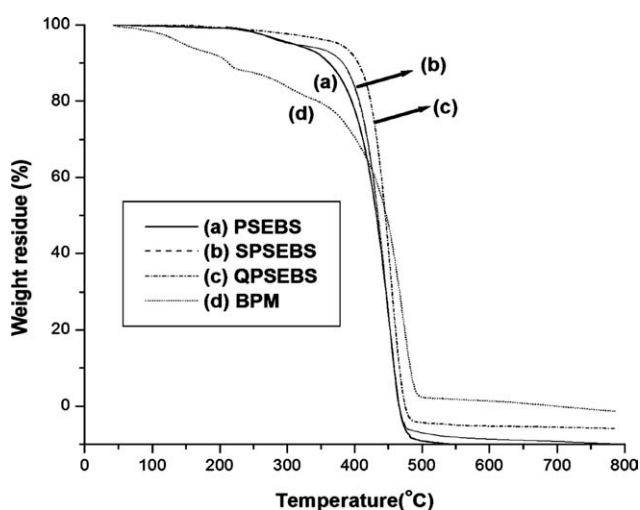


Figure 4. TGA curves of PSEBS (a), SPSEBS (b), QPSEBS (c), and BPM (d).

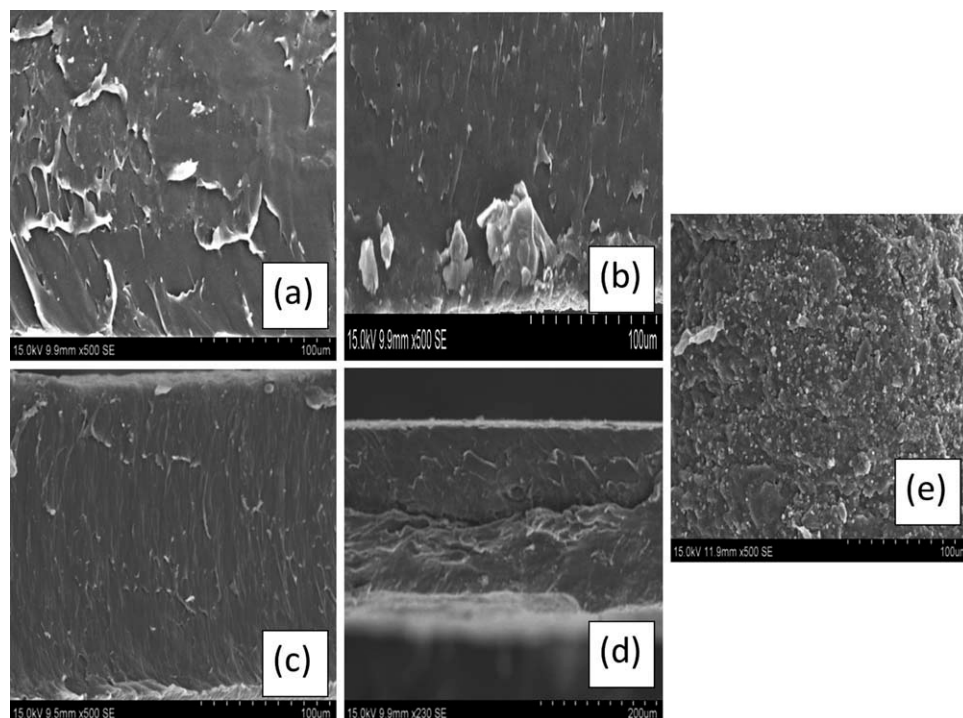


Figure 5. SEM photographs of the cross sectional views of PSEBS (a), SPSEBS (b), QPSEBS (c), BPM (d), and surface views of PVA on SPSEBS (e).

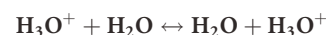
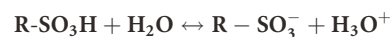
Determination of Water Absorption, IEC, and C_R

The IEC value for the prepared SPSEBS and QPSEBS were found to be 1.356 and 0.892 meq/g, respectively. The value 1.356 meq/g indicated the presence of acid group in polymer matrix which was responsible for the conduction of protons. Similarly, the IEC value of 0.892 meq/g indicated the presence of anionic channels which were responsible for the hydroxyl conductivity of the membrane.²⁴

Water uptake of SPSEBS, QPSEBS and BPM membranes, and C_R are shown in the Table I. The water absorption was determined by means of gravimetric techniques by measuring the increase in weight of the membranes following their immersion in water for 24 h.²⁵ In this case, the water absorption was measured every 4 h in a 24-h time period and was found to increase with time. From the data, it was inferred that SPSEBS showed much greater water absorption (286%) than BPM (235%) which was due to the hydrophilic nature of sulfonic acid group-

ings, whereas BPM comprised PVA and QPSEBS in addition to SPSEBS. In contrast, QPSEBS (3.33%) exhibited the least water absorption. The C_R was determined directly from the ratio of IEC to water absorption and expressed in M (mol/L).

Due to the high acidic nature of the sulphonic acid groups, it was expected that the interaction between water and sulphonic acid groups could give rise to H_3O^+ groups according to the reaction given below.²⁶ This interaction explained the rapid absorption of water.



Determination of co-ion Fluxes and Water Splitting Capacity

During current flow, hydrogen ions are generated at the anode and these ions carry almost the entire current across the CEL.

Table I. Physiochemical Properties of the Prepared Ion-Exchange Membranes

Time (h)	Water absorption (%)			Fixed group concentration (C_R)	
	SPSEBS (SD = 23)	QPSEBS (SD = 1)	BPM (SD = 5)	SPSEBS ($\times 10^{-3}$ M) (SD = 0.48)	QPSEBS (M) (SD = 0.93)
4	231	0.33	221	5.87	2.70
8	231	0.67	221	5.87	1.33
12	245	1.33	222	5.53	0.67
16	268	2.0	224	5.06	0.45
20	272	2.66	226	4.98	0.34
24	286	3.33	235	4.74	0.27

SD = Standard Deviation)

Therefore, if the BPM had operated at 100% current efficiency, the hydrogen ion and hydroxyl ion concentrations would have remained constant in the measured times. In fact, the current efficiencies of the BPM were less than 100%, on account of small leakage flows of Na^+ and Cl^- co-ions across the BPM. It was observed that while chloride accounted for the higher fraction of the co-ion transport of about 0.065, sodium ion accounted for 0.051 ion transport under similar experimental conditions.¹¹

The observed result of the water splitting effect getting accelerated when PVA was used as intermediate is a theoretical interpretation and was based on both protonation and deprotonation reactions model as well as hydrophilicity changes at the interface. Water splitting could be considered as a type of proton-transfer reaction occurring between water molecules and functional groups or chemicals.²⁷ The H^+ and OH^- were generated from protonation and deprotonation reactions between fixed charge groups on membrane and water molecules. As mentioned earlier, hydrogen bonding and polar interactions existed between PVA and water molecules which accelerated the water dissociation into H^+ and OH^- ions. In addition, PVA being highly hydrophilic, when it was coated over the membrane, the number of hydrophilic sites in the interfacial region increased as a result of adsorption. Correspondingly, efficiency of water splitting increased and the voltage across the BPM decreased. The water splitting capacity of SPSEBS-PVA-QPSEBS BPM was determined to be 0.88.²⁸

Determination of Permeate Flux, Water Dissociation Flux, and C-V Curve

Figure 6 shows the performance of the prepared BPM as a function of testing time. It was observed that with time, the water permeating flux decreased for the given feed solution. The water dissociation flux was observed to be 2.8×10^{-5} mol/m²/s and 2.2×10^{-5} mol/m²/s for acid (H^+) and base (OH^-), respectively. Figure 7 shows the current-voltage curve of the prepared

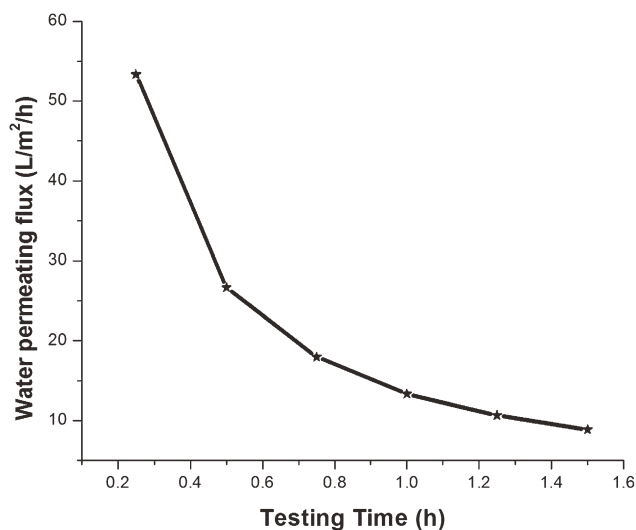


Figure 6. Membranes water permeation flux performance as a function of testing time.

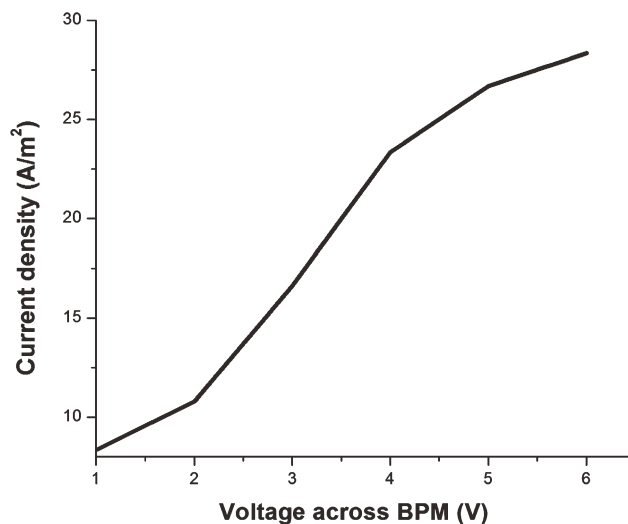


Figure 7. Current-Voltage curve of prepared SPSEBS-PVA-QPSEBS BPM (five-compartment electroalytic cell).

BPM with 50 g/L of NaCl concentration. The current-voltage curves due to water splitting have been used to examine the performance of a BPM⁵ and it usually reflects the electric property of the membrane. The current-voltage curve of the SPSEBS-PVA-QPSEBS BPM exhibited the typical behavior due to the coupling of electrical field which was enhanced by water dissociation which in turn was due to the chemical reaction and ion transport. Obviously, at small voltages, the current is carried by the salt ions displaying high resistance. In contrast, at high voltages, most of the current is carried by protons and hydroxyl ions dissociated from water and the resistance begins to decrease again with the applied voltage. The low water dissociation voltage that was observed from the curve suggests the immobilization of PVA in the IL as a result of its increasing hydrophilicity due to the attraction of water from the ion exchange layers to the space charge region. This indicated that the immobilized PVA functioned as a water dissociation catalyst.²⁹

CONCLUSION

The present report describes about the novel method developed for the preparation of inexpensive and chemically stable SPSEBS-PVA-QPSEBS BPMs which can be used for the separation of different types of ions from the wastewater. The main objective of this research work was to examine the capacity of synthesized membranes in terms of water dissociation flux, transport number, and permeation of fluxes which are essential for wastewater treatment. The prepared membranes were characterized in terms of TGA, water content, water splitting capacity, co-ion fluxes, and current-voltage relation. The preliminary study showed that the functional groups of PSEBS increased the water splitting effect and the phenomenon was explained due to the protonation-deprotonation reactions occurring between functional groups of PSEBS and the solvent molecules in the intermediate region of the BPM. Also, it was proved that the interface hydrophilicity was an important factor

in improving the water dissociation efficiency. Realizing the present growing trend and strict environmental norms enforced in discharging wastewater to the environment, it is appropriate to use the ED process for effective treatment of wastewater. Using membranes for the treatment of water to obtain purified water is potentially a large application of membrane technology today. This study further demonstrates the potential technological applicability of membranes for desalination of salt water under variable feed concentration. The advantage of such membranes over the commercial membranes in terms of cost factor and better performance would be favorable for their industrial application particularly in the treatment of saline and turbid water.

ACKNOWLEDGMENTS

Financial support from the Board of Research in Nuclear Science (BRNS), Mumbai, India (Letter. No. 2010/37C/1/BRNS/826, Dated: 28-06-2010) is gratefully acknowledged. Instrumentation facility provided under FIST-DST and DRS-UGC to Department of Chemistry, Anna University is sincerely acknowledged.

REFERENCES

- Sungkang, M.; Choi, Y. J.; Moon, S. H. *Korean J. Chem. Eng.* **2004**, *21*, 221.
- Cao, X.; Huang, X.; Liang, P.; Xiao, K.; Zhou, Y.; Zhang, X.; Logan, B. E. *Environ. Sci. Technol.* **2009**, *43*, 7148.
- Shannon, M. A.; Bohn, P. W.; Elimelech, M.; Georgiadis, J. G.; Marinas, B. J.; Mayes, A. M. *Nature* **2008**, *452*, 301.
- Nataraj, S. K.; Hosamani, K. M.; Aminabhavi, T. M. *Appl. Polym. Sci.* **2006**, *99*, 1788.
- Nataraj, S. K.; Sridhar, S.; Shaikha, I. N.; Reddy, D. S.; Aminabhavi, T. M. *Sep. Purif. Technol.* **2007**, *57*, 185.
- Wu, G. M.; Lin, S. J.; Yang, C. C. *J. Membr. Sci.* **2006**, *280*, 802.
- Nataraj, S. K.; Roy, S.; Patil, M. B.; Nadagouda, M. N.; Rudzinski, W. E.; Aminabhavi, T. M. *Desalination* **2011**, *281*, 348.
- Li, S. D.; Wang, C. C.; Chen, C. Y. *J. Membr. Sci.* **2008**, *318*, 429.
- Chen, R.; Hu, Y.; Chen, Z.; Chen, X.; Zheng, X. *J. Appl. Polym. Sci.* **2011**, *122*, 1245.
- Xue, Y. H.; Fu, R. Q.; Fu, Y. X.; Xu, T. W. *J. Colloid Interface Sci.* **2006**, *298*, 313.
- Gomez, H. E.; Lopez, L. Z. F.; Hernandez, E. R.; Martinez, M.; *J. Braz. Chem. Soc.* **2009**, *20*, 1294.
- Yang, B.; Zhang, H. *Front. Chem. China* **2008**, *3*, 10.
- Rongqiang, F.; Tongwen, X.; Weihua, Y.; Zhongxiao, P. *J. Appl. Polym. Sci.* **2003**, *90*, 572.
- Ji hua, H.; Cuixian, C.; Lin, L.; Lixin, Y.; Weijun, J. *J. Appl. Polym. Sci.* **2001**, *80*, 1658.
- Xu, C. X.; Chen, R. Y.; Zheng, X.; Chen, X.; Chen, Z. *J. Membr. Sci.* **2008**, *307*, 218.
- Michael Rajesh, A.; Kumar, M.; Shahi, V. K. *J. Membr. Sci.* **2011**, *372*, 249.
- Zhang, Y.; Xiao, C.; Liu, E.; Du, Q.; Wang, X.; Xu, H. *Desalination* **2006**, *191*, 291.
- Sachdeva, S.; Ram, R. P.; Singh, J. K.; Kumar, A. *AIChE J.* **2008**, *54*, 940.
- Sangeetha, D. *Int. J. Plastic technol.* **2004**, *8*, 313.
- Bhavani, P.; Sangeetha, D. *Energy*, **2011**, *36*, 3360.
- Sangeetha, D. *J. Polym. Res.* **2012**, *19*, 9824.
- Zeng, Q. H.; Liu, Q. L.; Broadwell, I.; Zhu, A. M.; Xiong, Y.; Tu, X. P. *J. Membr. Sci.* **2010**, *349*, 237.
- Vinodh, R.; Ilakkiya, A.; Elamathi, S.; Sangeetha, D. *Mater. Sci. Eng. B* **2010**, *167*, 43.
- Mani, K. N. *J. Membr. Sci.* **1991**, *58*, 117.
- Sondheimer, S. J.; Bunce, N. J.; Lemke, M. E.; Fyfe, C. A. *Macromolecules* **1986**, *19*, 339.
- Canovas, M. J.; Sobrados, I.; Sanz, J.; Acosta, J. L.; Linares, A. *J. Membr. Sci.* **2006**, *280*, 461.
- Fu, R. Q.; Xu, T. W.; Cheng, Y. Y.; Yang, W. H.; Pan, Z. X. *J. Membr. Sci.* **2004**, *240*, 141.
- Shi, S.; Lee, Y. H.; Yun, S. H.; Xuan Hung, P. V.; Moon, S. H. *J. Food Eng.* **2010**, *101*, 417.
- Jeevananda, T.; Yeon, K. H.; Moon, S. H. *J. Membr. Sci.* **2006**, *283*, 201.